

# Preparation and characterization of C/SiC–ZrB<sub>2</sub> composites by precursor infiltration and pyrolysis process

Haifeng Hu<sup>\*</sup>, Qikun Wang, Zhaohui Chen, Changrui Zhang, Yudi Zhang, Jun Wang

*CFC Lab, College of Aerospace and Materials Engineering, National University of Defense Technology, Changsha 410073, China*

Received 4 August 2009; received in revised form 2 September 2009; accepted 4 November 2009

Available online 29 November 2009

## Abstract

Ultra-high temperature ceramic matrix composites (C/SiC–ZrB<sub>2</sub>) are prepared by slurry and precursor infiltrations and pyrolysis method. C/SiC–ZrB<sub>2</sub> composites with ZrB<sub>2</sub> volume content from 10% to 24.6%, have balanced performance of fracture toughness (17.7–8.1 MPa m<sup>1/2</sup>), flexural strength at room temperature (367–163 MPa) and at high temperature (strength retention 74% at 1800 °C and over 32% at 2000 °C), better oxidation and ablation resistance under oxyacetylene torch environment (recession rate 0.01 mm/s).

© 2009 Elsevier Ltd and Techna Group S.r.l. All rights reserved.

**Keywords:** B. Composites; C. Mechanical properties; D. SiC

## 1. Introduction

Next generation hypersonic re-entry vehicles need ultra-high temperature materials as leading edges and nose caps to maintain sharp body to increase the lift-to-drag ratio so as to improve the vehicle performance in many ways [1]. Solid rocket engines, with ever-increasing higher chamber pressure and aluminium content, also need zero-erosion throat materials which must withstand temperature over 3000 °C. Ultra-high temperature ceramics (UHTC) are the most promising materials that stand up for these requirements and the most widely investigated systems. Numerous papers about components, processing, oxidation, and arc-jet ablation are published, and also flight experiment testified the application of UHTC [2].

Usually UHTC are prepared by hot-press sintering [3], pressure-less sintering [4], spark plasma sintering [5], reaction-sintering [6], etc., so these methods face the same difficulty of all bulk ceramics, that is, low fracture toughness (2–4 MPa m<sup>1/2</sup>) which limits thermal shock resistance property and also reliability. Furthermore, sintering process also limits preparation of large, complicated, thick parts.

Introduction of ceramic fiber to make ultra-high temperature ceramic matrix composites (UHTCMC) would improve greatly their fracture toughness and reliability. Previous papers reported carbon fiber reinforced composites with ZrB<sub>2</sub> or HfC as matrix, but with rather low fracture strength or low fracture toughness. Sayir [7] reported C/HfC composite preparation by chemical vapor infiltration process, but with flexural strength of only 26 MPa. Tang et al. [8] reported C/SiC–ZrB<sub>2</sub> fabrication by powder infiltration and CVI process, in which fracture toughness is about 5 MPa m<sup>1/2</sup> and ablation property is greatly improved compared with C/SiC composites under oxyacetylene torch ablation.

In this paper, carbon fiber cloth reinforced SiC–ZrB<sub>2</sub> composites (2D C/SiC–ZrB<sub>2</sub>) were prepared by slurry infiltration of ZrB<sub>2</sub> powders and precursor infiltration and pyrolysis (PIP) process to infiltrate SiC matrix, and their mechanical property, oxidation resistance property, and torch ablation property were investigated.

## 2. Experimental procedure

3K PAN-based plain carbon fiber cloth (Jilin Carbon Corporation, China) was used as reinforcement. Polycarbosilane (PCS), with molecular weight ~1300 and softening point ~210 °C, was synthesized in our laboratory. ZrB<sub>2</sub> powder with particle size ~2.5 μm and purity over 99.0% was used.

<sup>\*</sup> Corresponding author. Tel.: +86 731 84576441; fax: +86 731 84573165.

E-mail address: [hfhun@nudt.edu.cn](mailto:hfhun@nudt.edu.cn) (H. Hu).

The sample preparation is as follows. Firstly carbon fiber cloth was cut into 60 mm × 90 mm pieces, and then 12 pieces were vacuum infiltrated with the slurry (PCS/ZrB<sub>2</sub>/divinyl benzene (DVB)), stacked into a graphite mold, pressed to about 7 MPa, and cured in an oven at 150 °C for 2 h. Finally the sample together with the graphite mold was pyrolyzed up to 1200 °C in a furnace under flowing nitrogen atmosphere. Further densification was continued by repetition of vacuum infiltration of PCS/DVB solution, curing and pyrolysis. The C/SiC–ZrB<sub>2</sub> samples were labeled as ZB-0, ZB-20, ZB-30, ZB-40, ZB-50 and ZB-60 according to the volume ratios of ZrB<sub>2</sub> powder in slurry (the numbers indicated the volume fractions in percentage).

The apparent density was measured by Archimedes's method. Flexural strength ( $\sigma_f$ ) was determined using a three-point-bending test on specimens of 4.0 mm × 4.5 mm × 60 mm with 50 mm span and 0.5 mm/min crosshead speed. A single-edge-notched-beam (SENB) test was applied on notched specimen of 4.0 mm × 8.0 mm × 60 mm (notch with 0.3 mm in width and 4.0 mm in depth) with 0.05 mm/min crosshead speed and 30 mm span to determine fracture toughness ( $K_{IC}$ ). Over five samples were measured for the flexural and fracture toughness tests. The high temperature mechanical properties were tested on YKM2200 high temperature instrument (Northwestern Polytechnical University, China) with specimen size of 5 mm × 3.5 mm × 70 mm, span of 60 mm, crosshead speed of 0.597 mm/s, and only one sample was measured for each temperature.

Oxidation experiment was performed in a muffle furnace at 1200 °C. The sample was held for different time (20 min and 40 min) and then cooled down naturally to room temperature in air. Ablative resistance property test was carried out in a flowing oxyacetylene torch environment, with approximately 4187 kW m<sup>-2</sup> heat flux and ~3100 °C flame temperature. During the test, the specimen with a size of 30 mm × 30 mm × 5 mm, was vertically exposed to the flame. The distance between the nozzle tip and the surface of the specimen was 10 mm and the inner diameter of the nozzle tip was 2.0 mm. Over three samples were measured for oxidation and ablation tests.

The microstructure and composition of the samples were examined by scanning electron microscopy (JSM-5600LV, JEOL), and X-ray diffraction (Siemens D-500).

### 3. Results and discussion

#### 3.1. Microstructure and composition

Since the components (carbon fiber, ZrB<sub>2</sub> powder, and SiC matrix) were introduced step-by-step, and during preparation there exist weigh gain and weight loss, so it is important to determine exactly the contents of various components in the composite.

Assuming the ceramic yield of PCS is 65%, and that of DVB is 0 (small amount in slurry and low ceramic yield ~20%), so the following equations are presented to calculate the volume percentages of ZrB<sub>2</sub> powder ( $V_{ZrB_2}$ ), and SiC ( $V_{SiC}$ ) in the

composites, while that of carbon fiber ( $V_f$ ) can be determined from fiber mass and original sample volume.

$$V_{ZrB_2} = \frac{(m_1 - m_f)(m_{ZrB_2}/m_{ZrB_2} + m_{PCS}\eta)}{\rho_{ZrB_2} V_0} \times 100\%$$

$$V_{SiC} = \frac{\rho_0 - V_f \rho_f - V_{ZrB_2} \rho_{ZrB_2}}{\rho_{SiC}} \times 100\%$$

$V$ ,  $\rho$ ,  $m$  means volume percentage, density, mass, respectively, and subscript of 0, f, ZrB<sub>2</sub>, SiC, PCS means sample, fiber, ZrB<sub>2</sub> powder, SiC matrix, PCS, respectively.  $m_1$  means sample mass after first pyrolysis and  $\eta$  means ceramic yield of PCS.

According to the above equations, the volume percentage of the components in the composites were calculated and listed in Table 1.

From Table 1, the volume percentage of ZrB<sub>2</sub> in the composites increases with the increase of ZrB<sub>2</sub> content in the original slurry, and this value reaches 24.6% when ZrB<sub>2</sub> content in the slurry is 60%. When ZrB<sub>2</sub> content is too high, e.g., over 60%, the viscosity of the slurry is too high and slurry-infiltration of the carbon fiber cloth is impossible, so ZrB<sub>2</sub> content in the slurry, and thus ZrB<sub>2</sub> content in the composites, is limited.

It is also obvious that with ZrB<sub>2</sub> increase in the composites, the volume percentage of carbon fiber,  $V_f$ , decreases from 37.1% (without ZrB<sub>2</sub> introduction) to 18.9% (with 24.6% ZrB<sub>2</sub>), and  $V_f$  decrease will decrease mechanical properties of the composites. The reason for  $V_f$  decrease comes from the thicker matrix layer between two pieces of carbon fiber cloth due to higher content of ZrB<sub>2</sub> in the slurry, and at the same time,  $V_{SiC}$  remains almost at the same level (33%) in all C/SiC–ZrB<sub>2</sub> samples, except 48.7% for C/SiC (ZB-0) sample.

The density of the composites also logically increases with ZrB<sub>2</sub> increase, and reaches 2.59 g/cm<sup>3</sup> when ZrB<sub>2</sub> content in the slurry (ZrB-60) is 60%, compared with 1.87 g/cm<sup>3</sup> of C/SiC (ZB-0) composites. The difference would be much larger if C/SiC–ZrB<sub>2</sub> and C/SiC samples had the same porosity because the density of ZrB<sub>2</sub> (5.8 g/cm<sup>3</sup>) is much higher than that of SiC (3.2 g/cm<sup>3</sup>) as matrix. The porosity of C/SiC–ZrB<sub>2</sub> composites (~20%), is significantly higher than that of C/SiC (14.2%), indicating that ZrB<sub>2</sub> introduction is not beneficial for densification. And also trend is observed that higher content of ZrB<sub>2</sub> will cause higher porosity in the composites, which would be ascribed as the agglomerates of ZrB<sub>2</sub> particles and hindrance of PCS infiltration.

Table 1  
Contents of different components in C/SiC–ZrB<sub>2</sub> samples.

Sample	$\rho$ (g/cm <sup>3</sup> )	$V_{ZrB_2}$ (vol%)	$V_{SiC}$ (vol%)	$V_f$ (vol%)	Porosity (vol%)
ZrB-0	1.87	0	48.7	37.1	14.2
ZrB-20	2.06	10.0	33.8	35.9	20.2
ZrB-30	2.35	16.9	33.6	30.0	19.5
ZrB-40	2.46	19.4	35.4	25.7	19.6
ZrB-50	2.50	21.5	35.1	21.2	22.1
ZrB-60	2.59	24.6	33.2	18.9	23.3

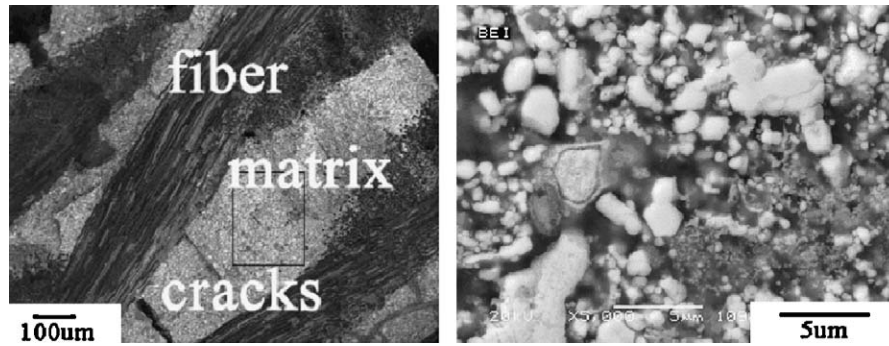


Fig. 1. SEM photos of the cut surfaces of C/SiC–ZrB<sub>2</sub> samples (a: layer structure, b: ZrB<sub>2</sub> particle (white) distribution).

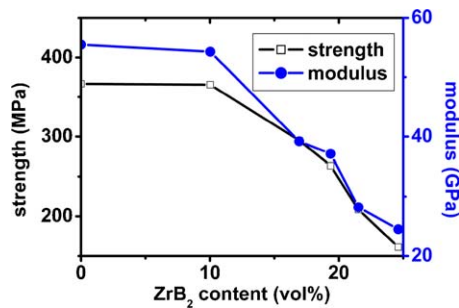


Fig. 2. The mechanical properties of C/SiC–ZrB<sub>2</sub> samples with different ZrB<sub>2</sub> contents.

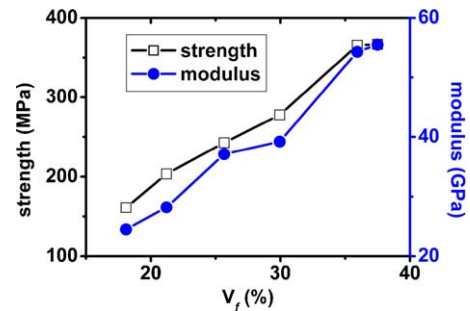


Fig. 3. The mechanical properties of C/SiC–ZrB<sub>2</sub> samples with different carbon fiber content.

The porosity is obvious in SEM photos, and layer-structure is observed as expected (Fig. 1). The ZrB<sub>2</sub> particles (white spots) distribute homogeneously in the matrix. It is very difficult to further increase density and decrease porosity by this slurry-infiltration and post-PIP process.

### 3.2. Mechanical property

The flexural strength and modulus of C/SiC–ZrB<sub>2</sub> composites are shown in Fig. 2. The flexural strength and modulus of the samples decrease almost linearly with ZrB<sub>2</sub> content increase, in which the flexural strength and modulus decrease from 367 MPa and 56 GPa of sample ZB-0 to 163 MPa and 24 GPa of sample ZB-60, respectively. This trend may be caused by (1) ZrB<sub>2</sub> introduction and/or (2) V<sub>f</sub> decrease, and or (3) porosity increase. Comparison of C/SiC (ZB-0) and C/SiC–ZrB<sub>2</sub> (ZB-20) indicates that small amount of ZrB<sub>2</sub> introduction does not influence fiber strength and fiber/matrix inter-phase, because two samples have almost the same flexural strengths, e.g., 367 MPa vs 366 MPa.

Further analysis (Fig. 3) shows that V<sub>f</sub> decrease causes almost linear decrease of flexural strength and modulus of the composites, showing that both SiC and ZrB<sub>2</sub> matrix contribute

only integral of the composites, and carbon fiber contributes mainly both strength and modulus.

Introduction of carbon fiber improves greatly fracture toughness of the samples (see Table 2), that is, 8.1–17.7 MPa m<sup>1/2</sup>, which is almost one order of magnitude higher than that of sintered ZrB<sub>2</sub> and ZrB<sub>2</sub>–SiC composites (2–4 MPa m<sup>1/2</sup>) [9]. This improvement shows significantly the advantages of C/SiC–ZrB<sub>2</sub> over sintered ZrB<sub>2</sub> ceramics, in that excellent thermal shock resistance under super-high ramping rate during re-entry, and also in the higher reliability of the composites, and also in the process availability of thick, complicated parts. Further study testified the excellent thermal shock resistance of the composites under ablation tests.

The mechanical properties of C/SiC–ZrB<sub>2</sub> composites at high temperatures were also measured and the results are summarized in Table 3. Sample of C/SiC–ZrB<sub>2</sub> (ZB-40) retained 74% of original strength and 51% of original modulus at 1800 °C, while sample of C/SiC retained only 35% of original strength and 58% of original modulus. It is obvious that introduction of ZrB<sub>2</sub> matrix improves greatly the mechanical properties at high temperature, mainly due to the higher melting point 3240 °C of ZrB<sub>2</sub> matrix (compared with decomposition point 2700 °C of SiC matrix). At 2000 °C sample of C/SiC–ZrB<sub>2</sub> still retained over 32% of

Table 2  
Fracture toughness of C/SiC–ZrB<sub>2</sub> composites.

Sample	ZB-0	ZB-20	ZB-30	ZB-40	ZB-50	ZB-60
K <sub>IC</sub> (MPa m <sup>1/2</sup> )	23.6 ± 4.3	17.7 ± 3.5	12.9 ± 2.1	10.5 ± 2.0	9.5 ± 1.5	8.1 ± 2.2



Table 3

Mechanical properties of sample ZB-40 and C/SiC (ZB-0) composites at high temperatures.

Sample		C/SiC–ZrB <sub>2</sub>	C/SiC
RT	$\sigma_f$ (MPa)	263	367
	$E$ (GPa)	35	56
1800 °C	$\sigma_f$ (MPa)	195 (74%)	118 (35%)
	$E$ (GPa)	18 (51%)	32 (58%)
2000 °C	$\sigma_f$ (MPa)	>84 (32%)	–
	$E$ (GPa)	15 (43%)	–



Fig. 4. The morphology of sample C/SiC–ZrB<sub>2</sub> (ZB-40) composites after flexural strength tests at high temperatures.

original strength and 43% of original modulus. Higher strength might be obtained because the sample did not break till the displacement limit of the instrument, and the sample showed significant displacement compared with the sample at 1800 °C (see Fig. 4), and this is in accordance with the decrease of modulus, indicating that ZrB<sub>2</sub> matrix showed softening phenomenon (stress-creep) over 2000 °C.

### 3.3. Oxidation property

The sample of C/SiC–ZrB<sub>2</sub> (ZB-40) and C/SiC were oxidized at 1200 °C for 20 and 40 min, after which the mass loss rate and flexural strength were determined (Table 4). Sample C/SiC–ZrB<sub>2</sub> after oxidation for 20 min, showed 4.5%

Table 4

Mass loss and flexural strength of C/SiC–ZrB<sub>2</sub> (ZB-40) and C/SiC before and after oxidation at 1200 °C.

Sample	Time (min)	Mass loss ratio (%)	$\sigma_f$ (MPa) Before (after) oxidation
C/SiC–ZrB <sub>2</sub>	20	4.5	266 (184, 69%)
	40	11.4	266 (141, 53%)
C/SiC	20	10.6	351 (71, 20%)

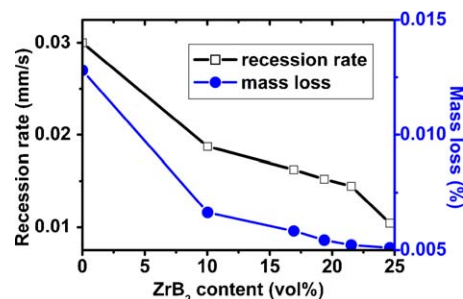
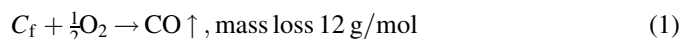
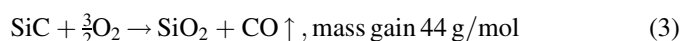
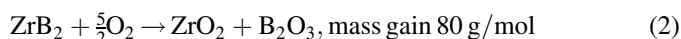


Fig. 6. Ablation properties of C/SiC–ZrB<sub>2</sub> samples.

mass loss, while C/SiC showed 10.6%. Further oxidation for 40 min sample C/SiC–ZrB<sub>2</sub> showed 11.4% mass loss. The mass change of C/SiC–ZrB<sub>2</sub> and C/SiC comes from two reasons. One is oxidation mass loss of carbon fiber, which can be described as follows.



The other is oxidation mass gain of ZrB<sub>2</sub> and SiC matrix, which is described as follows.



Both mass gain and loss contribute total mass loss of the sample, indicating as expected severe carbon fiber oxidation.

Besides the difference of mass loss, the flexural strength retention after oxidation of C/SiC–ZrB<sub>2</sub> and C/SiC is different, that is, after 20 min oxidation, the flexural strength retention of sample C/SiC–ZrB<sub>2</sub> is 69%, significantly higher than that of C/SiC (20%), indicating that introduction of ZrB<sub>2</sub> improves greatly the oxidation resistance of the composites. After exposition to oxidation for 40 min, the flexural strength

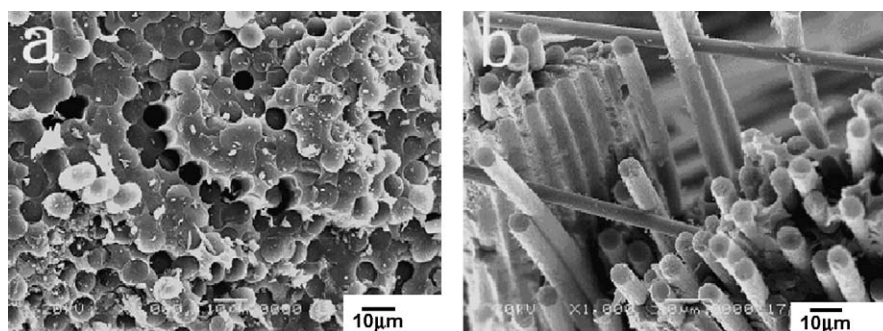


Fig. 5. SEM photos of interior fracture surfaces of the samples (a: C/SiC after oxidation, b: C/SiC–ZrB<sub>2</sub> after oxidation).

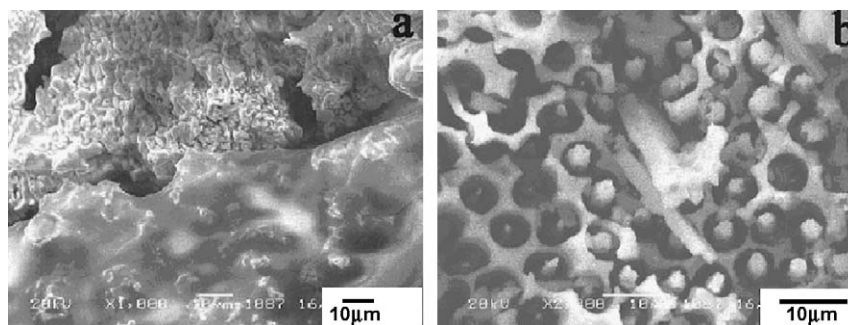


Fig. 7. SEM photos of the ablated surfaces of samples (a: sample ZB-40; b: C/SiC).

retention of C/SiC–ZrB<sub>2</sub> remains 53%, still higher than that of C/SiC. SEM analysis (Fig. 5) of the samples after oxidation also testifies severe oxidation of C/SiC, because interior fracture surface shows large amount of hollow holes due to carbon fiber oxidation and removal, while in case of C/SiC–ZrB<sub>2</sub> sample, carbon fiber pullout and rough fracture surface indicates oxidation did not progress into the interior and destroy the structure.

### 3.4. Ablation property

During the ablation test with oxyacetylene torch, the surface temperatures of the samples may reach values as high as 2300 °C after 8–10 s, and the mass loss rate and linear recession rate are shown in Fig. 6. When ZrB<sub>2</sub> content in the samples is raised from 0 to 10%, the mass loss rate is reduced from 0.013 g/s to 0.007 g/s, and linear recession rate is reduced from 0.03 mm/s to 0.018 mm/s, showing that introduction of ZrB<sub>2</sub> remarkably improves the ablation performance. Further increase of ZrB<sub>2</sub> content in the composites leads to slight decrease of mass loss rate and recession rate. With the highest content of ZrB<sub>2</sub> (24.5%) in the composites the mass loss rate and recession rate decrease accordingly to 0.005 g/s and 0.01 mm/s, respectively.

The ablation of the samples is mainly composed of three aspects: high temperature decomposition (destroy), oxidation, and gas evolution. The improvement of ablation property after ZrB<sub>2</sub> introduction is because (1) ZrB<sub>2</sub> matrix can withstand higher temperature due to high melting point (3240 °C), thus reducing high temperature decomposition (destroy).

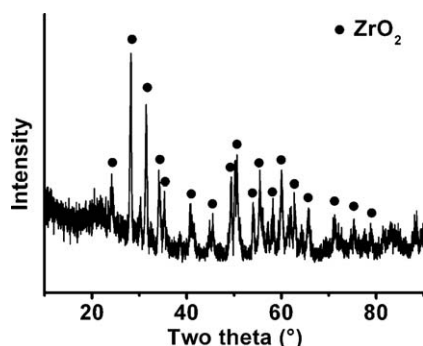


Fig. 8. XRD patterns of ZB-40 sample surface after ablation.

Considering that the surface temperature of the samples is as high as nearly 2400 °C, SiC matrix will tend to decompose and (2) ZrB<sub>2</sub> matrix has much better anti-oxidation property than SiC matrix, as proved both in the pure oxidation experiment at 1200 °C and in the analysis of ablation test. Further study of surface morphology after torch test shows that sample of C/SiC–ZrB<sub>2</sub> forms dense, glassy coating, while C/SiC cannot form glassy coating and shows priority of carbon fiber ablation and leaves hollow pores around tip-sharp carbon fiber (Fig. 7).

The dense, glassy coating is analyzed (Fig. 8), and mainly composed of ZrO<sub>2</sub>, obviously from oxidation of ZrB<sub>2</sub>. It is much strange that no SiO<sub>2</sub> exists in the surface coating, though existence of SiC matrix. The absence of SiO<sub>2</sub> may be due to the high temperature gas stream flowing away SiO<sub>2</sub> layer, which displays low viscosity at high temperature over 1800 °C (note that melting point of SiO<sub>2</sub> is 1710 °C). Same phenomenon is observed by other researchers in ablation tests of ZrB<sub>2</sub>–SiC composites, which is depletion of SiC in the outer surface of the sample [10]. At the same time, ZrO<sub>2</sub> forms viscous coating on the surface, thus decreasing the recession rate and protecting the fiber from further oxidation.

### 4. Conclusions

Ultra-high temperature ceramic matrix composites (C/SiC–ZrB<sub>2</sub>) were prepared by slurry-infiltration and precursor infiltration and pyrolysis method. Introduction of carbon fiber enhances fracture toughness up to 8.1–17.7 MPa m<sup>1/2</sup>, and introduction of ZrB<sub>2</sub> matrix improves greatly flexural strength at over 1800 °C, anti-oxidation property at 1200 °C, and anti-ablation property under oxyacetylene torch environment, compared with C/SiC composites. This method also has advantages in preparation of thick, complicated articles, compared with sintered bulk ceramics.

### References

- [1] M.J. Gasch, D.T. Ellerby, S.M. Johnson, Ultra high temperature ceramic composites, in: N.P. Bansal (Ed.), Handbook of Ceramic Composites, Kluwer Academic Publishers, Boston, USA, 2005 pp. 197–224.
- [2] W.G. Fahrenholtz, G. Hilmas, I.G. Talmy, J.A. Zaykoski, Refractory diborides of zirconium and hafnium, J. Am. Ceram. Soc. 90 (5) (2007) 1347–1364.
- [3] M. Gasch, D. Ellerby, E. Iiby, S. Beckman, M. Gusman, S. Johnson, Processing, properties and arc jet oxidation of hafnium diboride/silicon

- carbide ultra high temperature ceramics, *J. Mater. Sci.* 39 (2004) 5925–5937.
- [4] M. Quabdesselam, Z.A. Munir, The sintering of combustion synthesized titanium diboride, *J. Mater. Sci.* 22 (5) (1987) 1799–1807.
- [5] V. Medri, F. Monteverde, A. Balbo, A. Bellosi, Comparison of  $\text{ZrB}_2$ – $\text{ZrC}$ – $\text{SiC}$  composites fabricated by spark plasma sintering and hot-pressing, *Adv. Eng. Mater.* 7 (3) (2005) 159–163.
- [6] F. Monteverde, Progress in the fabrication of ultra-high-temperature ceramics: “in situ” synthesis, microstructure and properties of a reactive hot-pressed  $\text{HfB}_2$ – $\text{SiC}$  composite, *Comp. Sci. Tech.* 65 (2005) 1869–1879.
- [7] A. Sayir, Carbon fiber reinforced hafnium carbide composite, *J. Mater. Sci.* 39 (2004) 5995–6003.
- [8] S. Tang, J. Deng, S. Wang, W. Liu, Fabrication and characterization of an ultra-high-temperature carbon fiber-reinforced  $\text{ZrB}_2$ – $\text{SiC}$  matrix composite, *J. Am. Ceram. Soc.* 90 (10) (2007) 3320–3322.
- [9] F. Monteverde, A. Bellosi, S. Guicciardi, Processing and properties of zirconium diboride-based composites, *J. Eur. Ceram. Soc.* 22 (3) (2002) 279–288.
- [10] W.G. Fahrenholtz, Thermodynamic analysis of  $\text{ZrB}_2$ – $\text{SiC}$  oxidation: formation of a SiC-depleted region, *J. Am. Ceram. Soc.* 90 (1) (2007) 143–148.